

Electronic Whisker for Velocity Sensing Based on Liquid Metal Hysteresis Effect

Xinlong Sun^{1,‡}, Jun-Heng Fu^{1,2,‡}, Hongbin Zhao^{3,‡}, Wentao Xiang¹, Fei Zhan⁴, Chenkun Sun⁵, Shousheng Tang¹, Lei Wang^{1*}, Jing Liu^{1,6}

¹ Beijing Key Lab of Cryo-biomedical Engineering and Key Lab of Cryogenics, Technical Institute of Physics and Chemistry, Chinese Academy of Sciences, Beijing 100190, P. R. China

² College of Water Conservancy and Hydropower Engineering, Sichuan Agricultural University, Ya'an, 625014, P.R. China

³ State Key Laboratory of Advanced Materials for Smart Sensing, General Research Institute for Nonferrous Metals, Beijing 100088, P. R. China

⁴ School of Electrical and Electronic Engineering, Shijiazhuang Railway University, Shijiazhuang, Hebei, 050043, P. R. China

⁵ Department of Chemical and Physical Science, University of Toronto Mississauga, L5L 1C6, Canada

⁶ Department of Biomedical Engineering, School of Medicine, Tsinghua University, Beijing 100084, P. R. China

[‡] These authors contributed equally to this work

* Corresponding Author: leiwang@mail.ipc.ac.cn

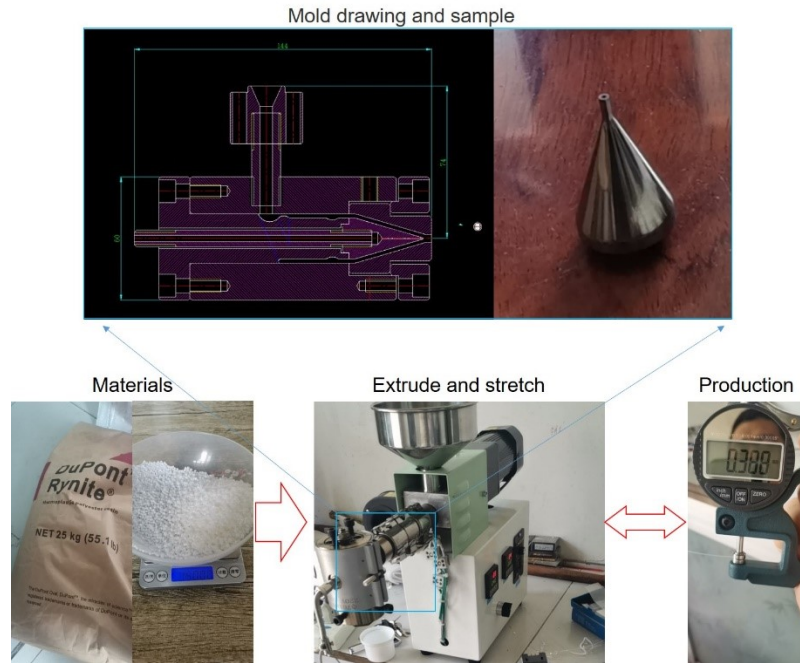


Figure S1. The process to produce hollow fiber, applying the extrusion molding technology. The diameter of hollow fiber can be controlled ranging from 120 μm - 260 μm .

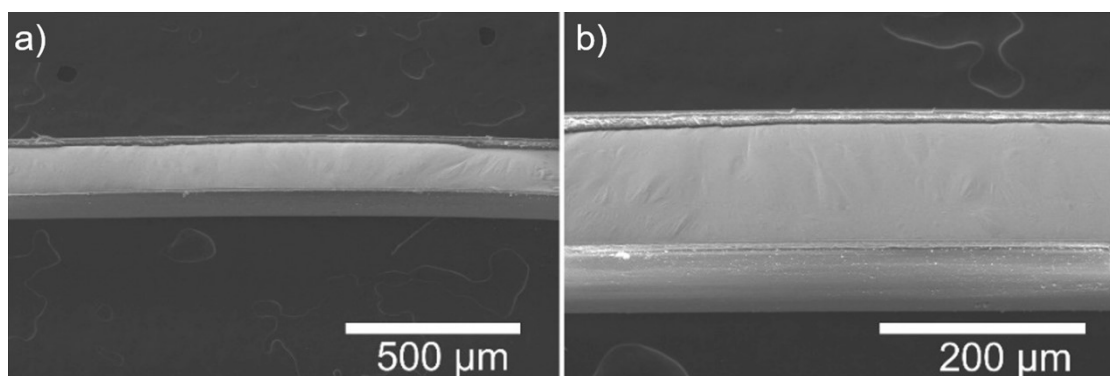


Figure S2. The internal state of integrated fiber after injecting liquid metal. The liquid metal uniformly fills with the hollow fiber.

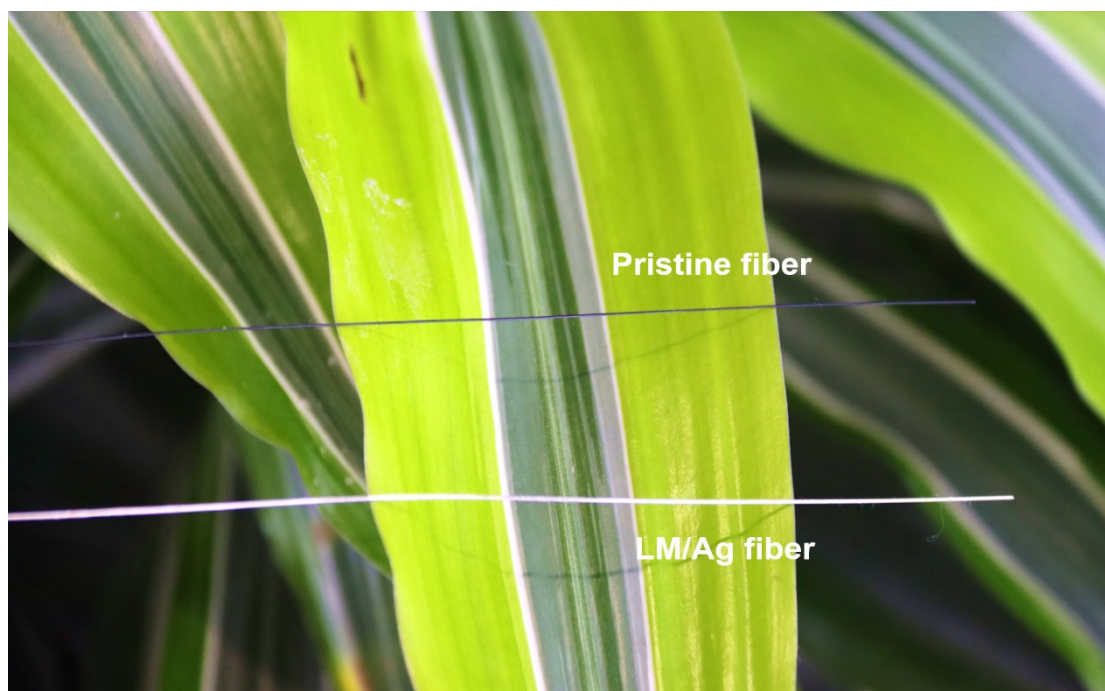


Figure S3. The optical image of pristine hollow fiber (upper) and integrated fiber sensor (lower).

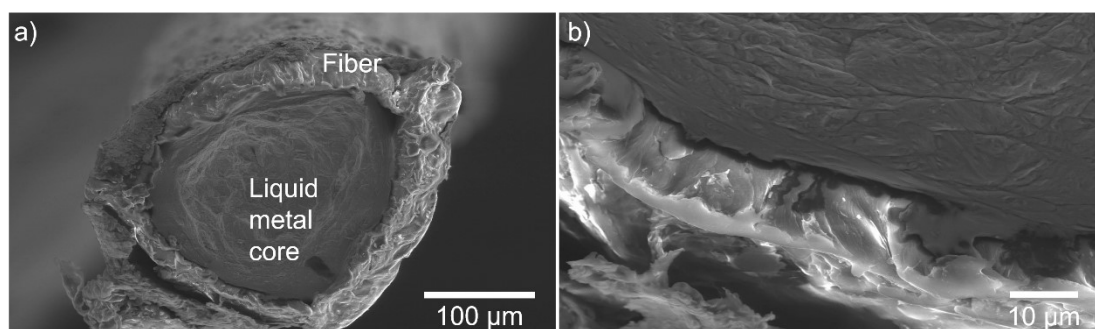


Figure S4. The cross-section of the as-made e-whisker and partial enlarged detail, where the liquid metal adhered closely to fiber and no leakage was found.

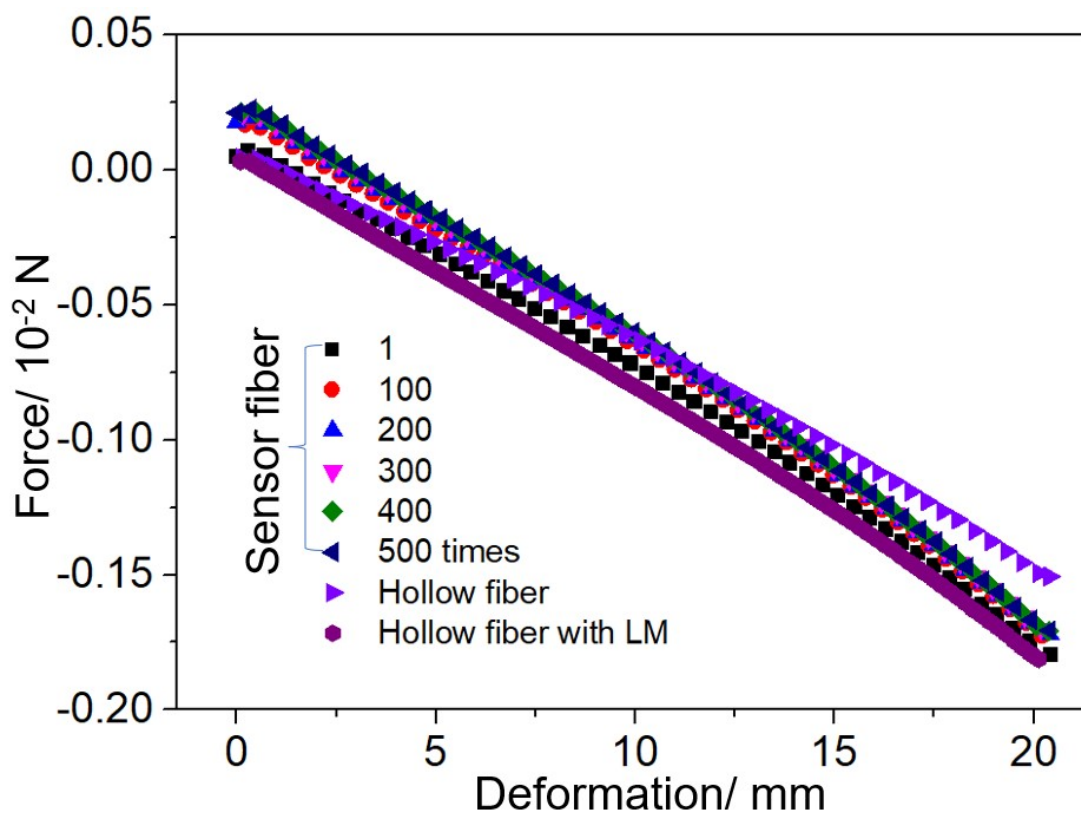


Figure S5. Reversibility of sensor fiber after mechanical external force cycle under the condition of the bending by 12.5° . The mechanical properties of fiber were recorded in every 100 times. No obvious changed under hundreds of cycles. In addition to integrated sensor fiber, the original hollow fiber and that one injected with liquid metal were also recorded as hollow fiber and hollow fiber with sensor respectively.

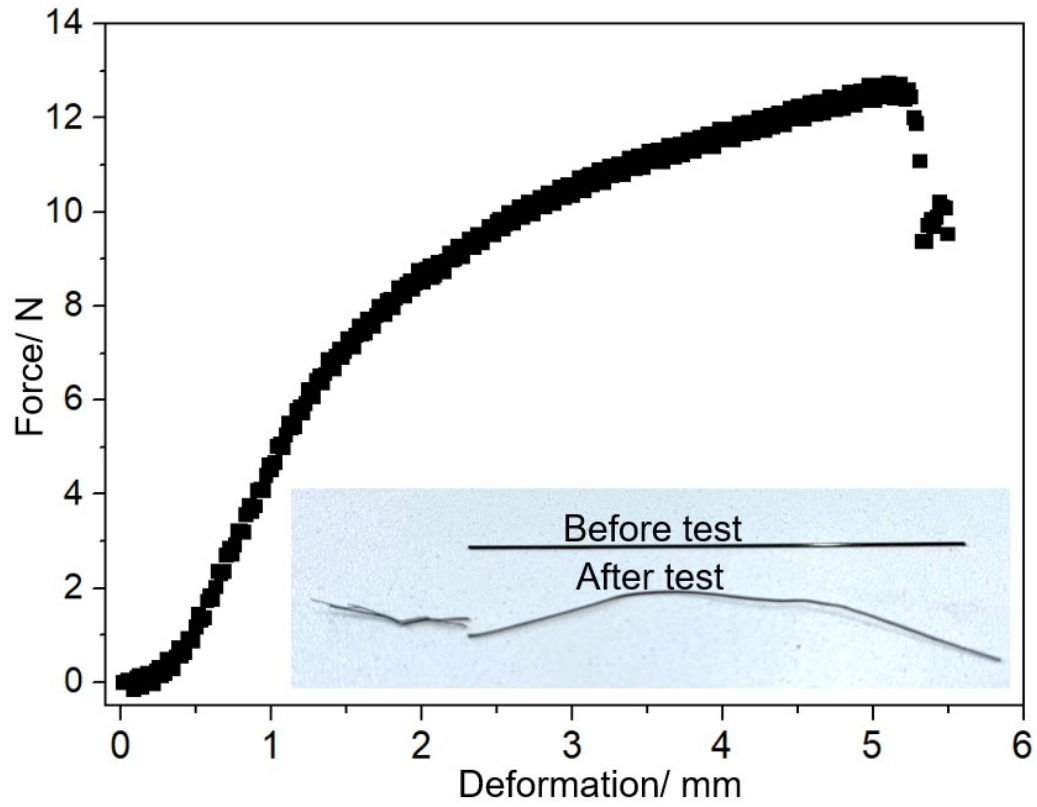


Figure S6. The extension test. It is non stretchable.

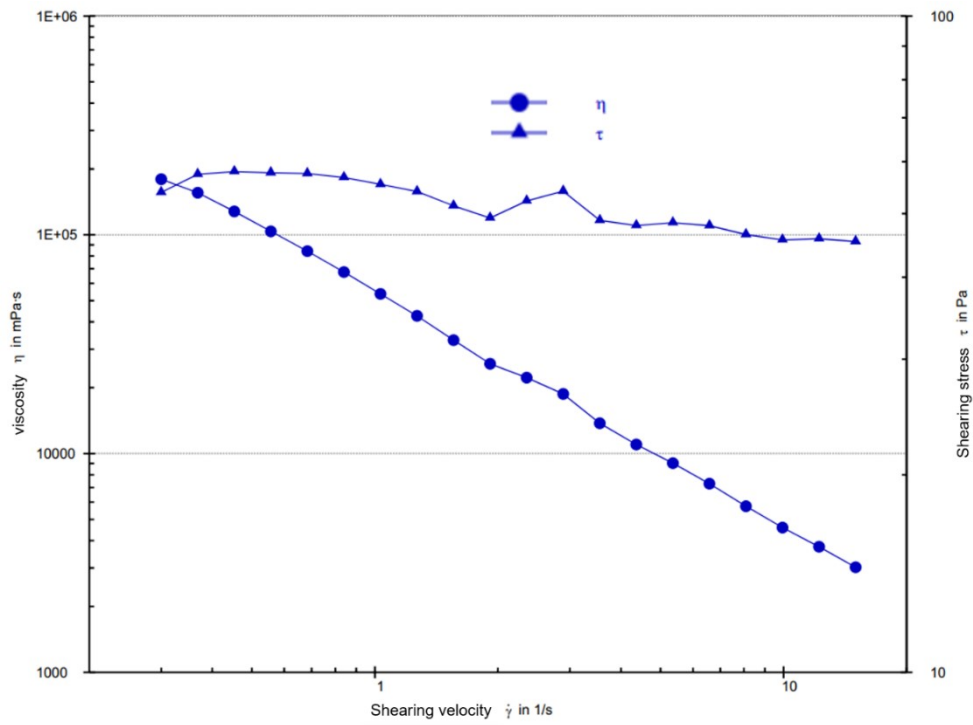


Figure S7. The viscosity tests.

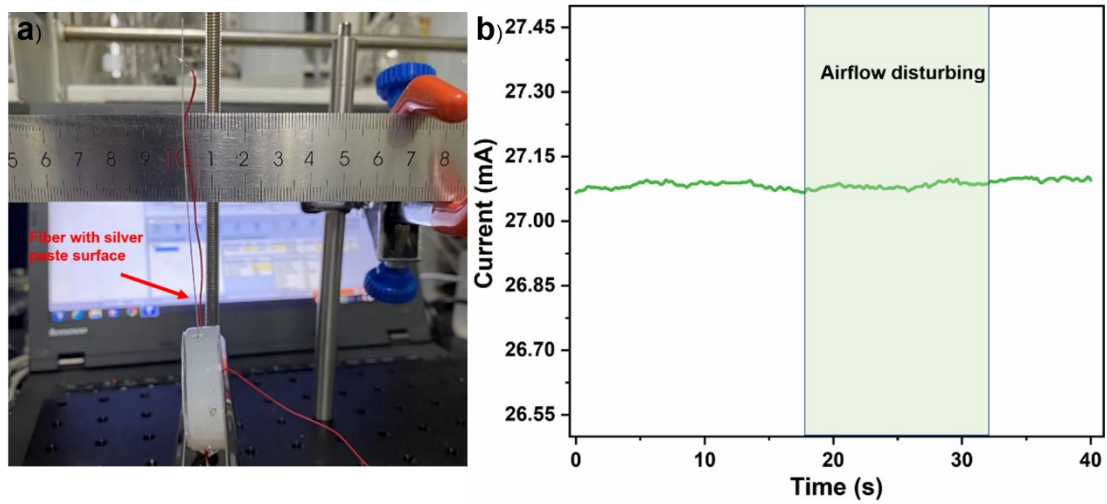


Figure S8. The test of the effect of the silver layer toward resistance change

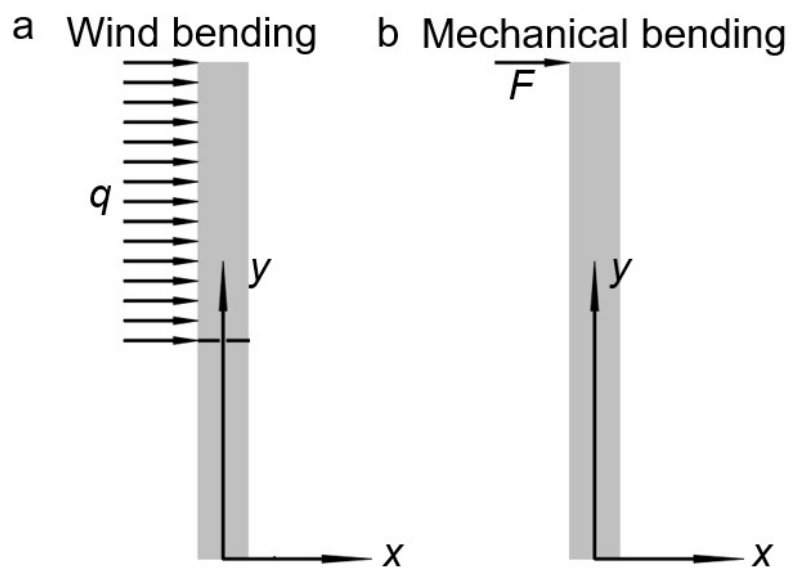


Figure S9. Two forms of external force applied to the fiber: wind bending and mechanical bending. a) The wind acts vertically on the upper part of the fiber. b) The mechanical force is applied vertically to the tip of the fiber.

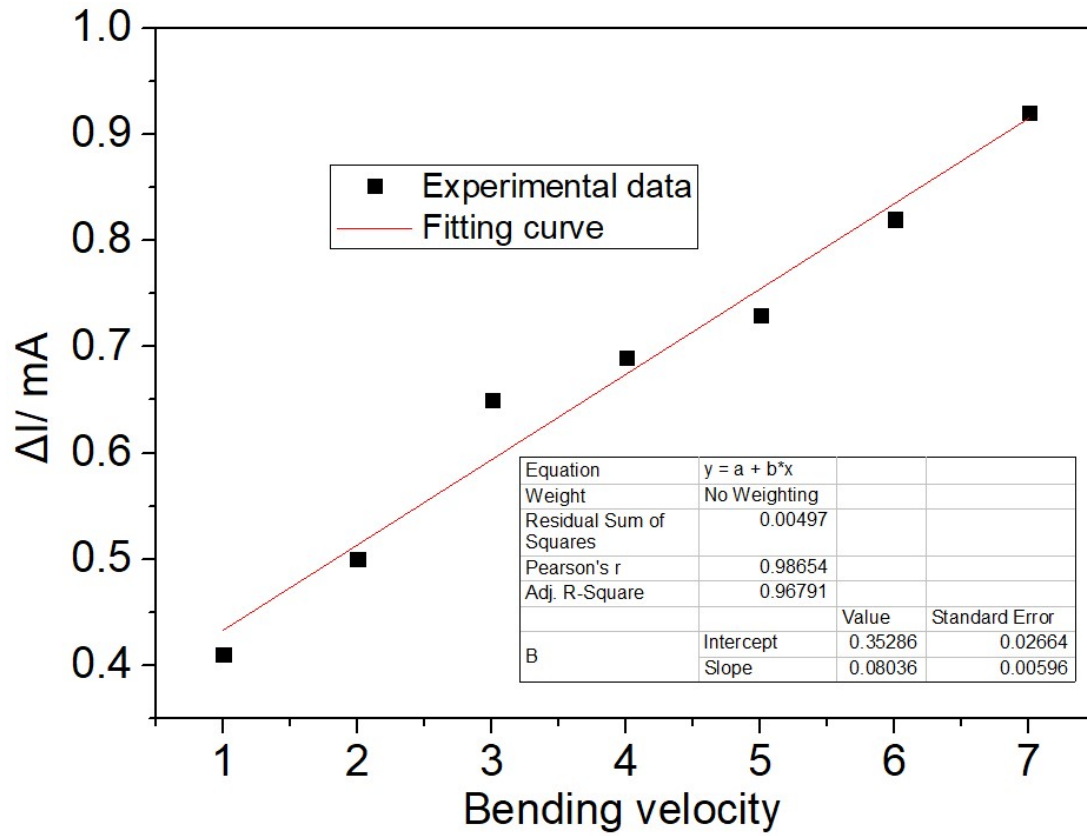


Figure S10. The relationship between the mechanical bending velocity generated by running remote controlled car and the current change. The relationship is linear with goodness of fit reaching to 96.79%.

Table S1. Parameters used in the simulation.

surface tension	0.072 N/m
gravitational acceleration	9.8 m/s ²
liquid density	6900.0 kg/m ³
liquid viscosity	0.001003 kg/(m×s)
gas density	1.225 kg/m ³
gas viscosity	0.001003 kg/(m×s)
contact angle	150 deg
drop radius	2.0 mm
time step	0.0001 s
fiber density	1000 kg/m ³
fiber poisson's ratio	0.38
fiber elastic modulus	1 GPa

Table S2. Parameters of liquid metal in the viscosity test

Data number	Shearing rate	Shearing strain	Shearing stress	Viscosity	Torque	Normal force
	[1/s]	[%]	[Pa]	[mPa·s]	[mN·m]	[N]
1	0.3	75.6	53.868	1.80E+05	0.24727	0.14
2	0.369	243	57.397	1.56E+05	0.26347	0.11
3	0.453	450	57.939	1.28E+05	0.26596	0.09
4	0.556	703	57.695	1.04E+05	0.26484	0.07
5	0.683	1.01E+03	57.543	84192	0.26414	0.05
6	0.84	1.40E+03	56.755	67579	0.26052	0.05
7	1.03	1.87E+03	55.401	53693	0.25431	0.05
8	1.27	2.45E+03	54.03	42617	0.24802	0.03
9	1.56	3.16E+03	51.392	32993	0.23591	0.01
10	1.91	4.03E+03	49.24	25729	0.22603	0
11	2.35	5.10E+03	52.276	22233	0.23997	0.03
12	2.89	6.42E+03	54.097	18725	0.24832	0.06
13	3.55	8.04E+03	48.833	13756	0.22416	0.01
14	4.36	1.00E+04	47.957	10996	0.22014	0.02
15	5.36	1.25E+04	48.435	9038	0.22233	0.03
16	6.58	1.55E+04	47.933	7280.6	0.22003	0.02
17	8.09	1.92E+04	46.462	5743.2	0.21328	0.01
18	9.94	2.37E+04	45.599	4587.4	0.20931	0.01
19	12.2	2.93E+04	45.788	3749.3	0.21018	0.02
20	15	3.62E+04	45.336	3021.3	0.20811	0.02